The Residual Strength of Fiber-Reinforced EPS Lightweight Concrete after Exposure to Fire

Alaa A. Abd
Department of Civil Engineering, College of Engineering, University of Baghdad, Baghdad, Iraq
alaa.salman2201m@coeng.uobaghdad.edu.iq (corresponding author)

Rafaa M. Abbas
Department of Civil Engineering, College of Engineering, University of Baghdad, Baghdad, Iraq
dr.rafaa@coeng.uobaghdad.edu.iq

Received: 4 June 2025 | Revised: 9 July 2025 | Accepted: 13 July 2025

 DOI: https://doi.org/10.48084/etasr.12547

ABSTRACT

Aggregates typically constitute 65%-75% of the concrete volume and significantly influence its mechanical properties while also playing a crucial role in the post-fire behavior. This study explores the effect of fire exposure on thermal conductivity, residual strength, and performance of Expanded Polystyrene (EPS) lightweight Self-Compacting Concrete (SCC) reinforced with steel fibers. EPS beads are utilized as a coarse aggregate replacement and steel fiber reinforcement with different volume fractions. The test for the pre-fire concrete samples indicated that EPS beads significantly reduced the mechanical properties of the hardened concrete, resulting in significant improvement in the splitting and flexural strength due to the steel fiber reinforcement. Also, the rheological properties for the mixtures were within the ENFARC limits for the different EPS and fiber volume fractions. Following exposure to fire, the findings revealed that increasing the EPS content enhances the retention of strength in the post-fire samples. The experimental results highlighted the constructive effect of EPS beads on tensile strength, flexural strength, and mass loss due to fire exposure. On the other hand, for post-fire performance, results revealed a significant adverse effect of the steel fibers on the thermal conductivity and mechanical properties of the concrete samples.

Keywords-lightweight concrete; Expanded Polystyrene (EPS); elevated temperature; fiber reinforced; Self-Compacting Concrete (SCC); thermal conductivity

I. INTRODUCTION

One of the main disadvantages of conventional concrete is its considerable self-weight. The density of standard concrete typically ranges from 2200 kg/m³ to 2600 kg/m³, making it an economically unfavorable material when considering casting molds, thickness, and reinforcement for foundation. Lightweight concrete is a type of concrete that has a density ranging from 300 kg/m³ to 1850 kg/m³ [1, 2]. For a lightweight concrete to be effectively used in buildings, it must possess specific characteristics that fulfill the required standards for strength and performance in the application. Prior to the use of any material in construction, it is essential to investigate its mechanical properties to assess its suitability. Due to its low density, which provides significant advantages by reducing the size of components, the demand for lightweight concrete has increased in many architectural projects [2].

Reusing and recycling waste materials is the most eco-friendly solution to the disposal issue. Consequently, a new method for producing lightweight concrete involves using lightweight materials, such as agricultural waste, construction waste, and corks, as substitutes for aggregates (either coarse or fine) [3]. EPS is one such material, which has acquired a broader use in modern construction. EPS is a very lightweight waste material generated from industry and used consumer products. The waste disposal problem can be solved by using waste EPS as a recycled material to produce sustainable lightweight concrete by substituting conventional aggregates [4, 5]. EPS lightweight concrete has found applications in constructing structural elements, such as beams, walls, and slabs, owing to its lightweight characteristics and advantageous thermal properties [6]. Authors in [7, 8] investigated the mechanical properties of concrete mixed with a high-strength cement matrix and EPS particles. The study developed a model that links the concrete strength with the size and content of the EPS particles. When concrete is subjected to fire and elevated temperatures, the microstructure and properties of the cement hydration products alter with the temperature changes, which directly or indirectly compromise the macroscopic properties of the matrix, thus affecting the overall behavior of the concrete at high temperatures [9]. As the fire temperature reaches 200°C or higher, the decomposition of cement hydrates and the deterioration of aggregates begin in the concrete. The disparity in the thermal expansion between the cement matrix and the aggregates results in stress concentration, leading to a substantial decline in concrete strength, with the extent of strength reduction depending on both the properties of the

aggregate and the temperature experienced by the concrete [10]. In environments where temperatures escalate rapidly, High-Strength Concrete (HSC) is more prone to spalling due to the combined effects of pore pressure and thermal stress resulting from temperature gradients during heating [11, 12]. This severely compromises the structural integrity of reinforced concrete structures, making the spalling behavior of HSC at elevated temperatures a topic of considerable interest [13, 14].

Fibers have been used as reinforcement. In fiber-reinforced concrete, the thermal interface between the fibers and the concrete matrix may result in thermal cracking when exposed to high temperatures. Authors in [15] conducted a data-driven analysis of real fire tests, revealing that the artificial intelligence technology serves as a powerful tool for precisely predicting fire-induced spalling phenomena. Authors in [16] examined the residual strength of HSC after exposure to elevated temperatures. Their experimental findings revealed that HSC is susceptible to explosive spalling after high-temperature exposure, with early spalling occurring around 400°C. Authors in [17] reviewed the mechanical properties of Steel Fiber-Reinforced Concrete (SFRC) subjected to high temperatures. Their detailed analysis highlighted that SFRC generally demonstrates superior residual mechanical properties compared to the plain concrete under high-temperature conditions. Authors in, [18] examined the contribution of EPS particles on fire resistance, thermal properties, and compressive strength of foamed concrete. The results indicated that the increasing EPS bead content lowers the thermal conductivity, strength, and fire endurance of foamed concrete. An investigation on the impact of high temperature on normal and high-strength lightweight SCC, incorporating Perlite, Scoria, and Polystyrene aggregates, showed that the strength and thermal stability of lightweight concrete made from such aggregates change after the exposure to high temperatures [19]. Authors in [20] focused on developing sustainable, fire-resistant concrete by incorporating EPS beads. A lightweight, HSC was developed by replacing 50 % of the sand volume with EPS. The findings exposed the performance of EPS-infused HSC, highlighting its role in enhancing the thermal characteristics due to fire exposure. The lightweight concrete is a popular material in the construction industry due to benefits, involving low thermal expansion, heat, and sound insulation capabilities.

This study examines pre-fire and post-fire behavior of fiber-reinforced lightweight concrete with EPS beads as a coarse aggregate. The experimental program involved the casting and standardize testing of concrete samples to explore the residual strength of lightweight concrete made using different proportions of coarse aggregate substituted with EPS beads (i.e., 20% and 40%) and reinforced with various volume fractions of steel fiber (i.e., 0%, 0.5%, and 1%). The assessment was conducted before and after exposure to steady-state fire at 700°C. The concrete's performance was assessed based on its residual mechanical properties, such as compressive strength, tensile strength, flexural strength, mass loss, and thermal conductivity.

II. EXPERIMENTAL PROGRAM

A set of standard test specimens was selected to achieve the study objectives. The 28-day compressive strength was studied using 150 mm ×150 mm ×150 mm cubes. Tests on split tensile strength were performed on 150 mm × 300 mm cylindrical specimens. The flexural strength was measured using prisms measuring 500 mm ×100 mm ×100 mm. The thermal conductivity was examined using 100 mm ×100 mm ×100 mm cubes. Seven concrete mixtures were designed, and for each mix, 3 cubes, 2 cylinders, and 2 prisms were cast, considering twice the number of samples required for both the burned and unburned cases. Eventually, a set of 42 cubes, 28 cylinders, and 28 prisms were cast.

A. Materials

In this study, SCC complying with the specifications and guidelines provided by EFNARC (2005) [21] served as the basis for the mix design. SCC is a highly fluid and non-segregating concrete that can flow easily under its own weight, filling narrow spaces without mechanical vibration. The materials utilized for producing the SCC mixture included Portland cement, natural coarse and fine aggregates, silica fume, and a superplasticizer. Superplasticizers are used to increase the fluidity of concrete without adding excess water and to avoid the segregation of EPS spheres in the concrete. To achieve low-density concrete in the experimental phase, EPS beads were incorporated to replace a certain percentage of the aggregate, specifically 20% and 40% of the coarse aggregate's volume fraction. To improve the strength characteristics of the final EPS mixture, various proportions of hooked steel fibers were utilized. The mechanical properties of the hooked steel fibers are detailed in Table I, while Table II presents the composition and proportions of SCC materials for the different mix designs.

TABLE I. MECHANICAL PROPERTIES OF STEEL FIBER

Fiber size, *D* (mm)	**Length, *L* (mm)**	**Fiber aspect ratio (*L/D*)**	**Yield strength (MPa)**
0.5	50	100	1900

TABLE II. MIXTURE COMPOSITION AND PROPORTIONS FOR DIFFERENT MIXTURES

Mix Designation	**Mix Proportions (kg/m^3)**						**SP (lit/m^3)**	**Silica fume** (%)**
	SF	**EPS***	**Gravel**	**Sand**	**Cement**	**Water**		
R	185	441	750	950	0	0	4	4
EPS20SF0	185	441	750	760	2	0	4	4
EPS20SF0.5	185	441	750	760	2	39	4	4
EPS20SF1	185	441	750	760	2	78	4	4
EPS40SF0	185	441	750	570	4	0	4	4
EPS40SF0.5	185	441	750	570	4	39	4	4
EPS40SF1	185	441	750	570	4	78	4	4

* Replacement by volume of coarse aggregates, ** Content by weight of cement.

B. Concrete Mixing, Casting, and Curing

A mechanical pan-type mixer with a capacity of 0.25 m³ was employed to blend the concrete components. Initially, 40% of the water, along with the superplasticizer, was added to the mixer, followed by the dry EPS particles. The mixing continued for approximately 2 min to ensure that the EPS particles were thoroughly wet with water and superplasticizer. Next, the solid components were introduced into the mixer, with the remaining 60% of the water being gradually added. Finally, the fibers were evenly distributed throughout the mixture, and the mixing was resumed for an additional 2 min. Subsequently, the fresh fiber-reinforced EPS lightweight concrete was poured into molds. A steel trowel was utilized to create leveled and smooth surfaces on the specimens. Finally, concrete cubes, cylinders, and prisms were removed from their molds 24 h after casting and transferred for 28 days of curing using wet burlap.

C. Burning and Cooling

The specimens were subjected to burning in a gas furnace using direct fire, while maintaining controlled conditions, specifically a steady-state temperature of 700 ± 10 °C for an exposure duration of 1 h, as illustrated in Figure 1.

(a) (b)

Fig. 1. Burning samples, (a) molds in the furnace, (b) temperature control.

A digital thermometer with a K-type sensor wire was utilized to monitor and record the fluctuations within the furnace environment over time. The criteria for the temperature-time relationship were established based on ASTM E-119 standard [22]. The change in temperature during the fire test was divided into three stages: heating to 700 °C (10 min), followed by constant temperature at 700 °C (60 min), and after that cooling to ambient temperature [23, 24]. During the heating stage, the furnace was heated in accordance with ASTM E119-20.

III. RESULTS AND DISCUSSION

A. Fresh Concrete Tests

Several trial mixes were performed to produce SCC with a target cube compressive strength of approximately 57 MPa. The mix proportions for the *R* mix, as detailed in Table II, represent the reference SCC mix. Various tests were conducted to evaluate the rheological properties of the adopted mix, including slump flow time (T500), maximum slump diameter, L-box flow times, and V-funnel flow times. To assess the flowability of SCC, the slump flow time and the diameter of the spread area are typically utilized [25]. The results indicated that the slump flow time for the *R* mix was 1.8 sec. According to EFNARC (2005) [21], a slump flow time of ≤ 2 sec is required for viscosity class VS1. The slump flow diameter of 730 mm fell within the acceptable range for the slump flow class SF2 (660 mm - 750 mm), making it suitable for many standard applications. The L-box test demonstrated a blocking ratio of 0.889 for the *R* mix, confirming the compliance with EFNARC's passing ability limits of ≥ 0.8 for PA1 or PA2 classes.

The V-funnel flow time measured at 5 sec was also within the VF1 flow time limit of ≤ 8 sec, as outlined by EFNARC, thus all test results for the *R* mix confirmed that the concrete mix is qualified as SCC. Furthermore, the results of the slump flow test, T500 time, V-funnel flow time, and L-box tests for the mixes where only the coarse aggregate was replaced with EPS (i.e., EPS20FS0 and EPS40FS0) were also within the acceptable ranges set by EFNARC, indicating that the EPS content does not adversely impact the rheological properties of the SCC mixes. However, the addition of steel fibers to the mixes (i.e., EPS20FS0.5, EPS20FS1, EPS40FS0.5, and EPS40FS1) reduced the workability, though it remained within the EFNARC limits. These findings suggest an inverse relationship between the quantity of steel fibers added to the mix and the workability of the concrete, indicating that the flowability of SCC containing steel fibers is reduced when moving through confined spaces.

B. Hardened Concrete Tests

1) Density and Mass Loss

The mass of concrete decreases with an increasing temperature due to the moisture evaporation, spalling, and fracture of the concrete surface. The mass loss for each concrete mix is presented in Table III. As anticipated, the proposed EPS mixes showed a decrease in weight in relation to the amount of EPS content used due to replacing heavy gravel particles with lightweight EPS beads. The results for the reference mix (R) indicated a density of 2485 kg/m³, consistent with Normal Weight Concrete (NWC), as specified by ACI 318-19 [26]. However, after fire exposure, the observed mass was 2262 kg/m³ revealing a mass loss of 8.9%. The data from the first group showed that using 20% EPS resulted in density reductions of 14.8%, 14.6%, and 10.7% for the steel fiber contents of 0%, 0.5%, and 1%, respectively. In the second group, where 40% EPS was used, the density of the concrete decreased by 20%, 18%, and 14.6%, respectively, compared to using 0%, 0.5%, and 1.5% steel fibers. The decrease in density reduction corresponding to increasing the steel fiber percent is expected due to the high density of the added steel fiber, i.e. 7850 kg/m^3, highly contributing to concrete density [4, 27].

The results for the mass loss due to fire exposure demonstrated an inverse relation between the amount of EPS aggregate added and the mass loss with the temperature increase. This is justified by the reduced risk and severity of spalling, which diminishes as the content of lightweight aggregate rises due to its thermal insulation features [20]. This

conclusion is consistent with the findings for concrete with 0.5% and 1% of steel fiber. However, the mass loss has slightly increased for non-fibrous concrete (0% steel fiber) with increasing EPS. This result might be attributed to inaccurate test measurements. The mass loss for each concrete mix is illustrated in Figure 2 and Table III. After exposure to a steady-state temperature of 700°C, the observed mass loss percentages were 8.9%, 4.1%, 7.6%, 9.3%, 4.8%, 7.1%, and 8.6% for the respective EPS replacement ratios for R, EPS20SF0, EPS20SF0.5, EPS20SF1, EPS40SF0, EPS40 SF0.5, and EPS40SF1. Moreover, the results presented in Table III indicated an additional increase in the mass loss when incorporating steel fiber in the concrete mixes. This fact is due to the high thermal conductivity of steel fibers that mitigate the EPS thermal insulation and, thus, accelerate the water evaporation and concrete spalling losses.

TABLE III. PERCENTAGE OF MASS LOSS

Mix designation	Unburned samples, (kg/m^3)		Burned samples, (kg/m^3)	
	Density	%Reduction	Density	%Mass loss
Group one				
R	2485	----	2262	8.9
EPS20SF0	2117	14.8	2031	4.1
EPS20SF0.5	2122	14.6	1928	7.6
EPS20SF1	2218	10.7	2012	9.3
Group two				
R	2485	----	2262	8.9
EPS40SF0	1988	20.0	1891	4.8
EPS40SF0.5	2013	18.0	1869	7.1
EPS40SF1	2120	14.6	1937	8.6

2) *Compressive Strength*

The results from this test were determined based on the average compressive strength of three cubes before and after burning, each measuring 150 mm ×150 mm ×150 mm. Table IV presents the residual compressive strength of the tested specimens. The results for the reference mix (R) indicated a reduction of 31.7% in the compressive strength due to fire exposure. This finding showed the severe decline in the compressive strength when concrete is exposed to high temperatures with no additives [18].

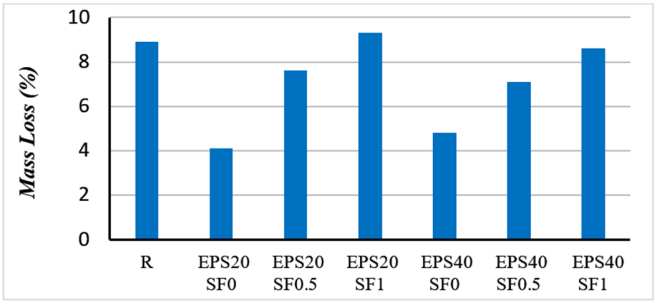

Fig. 2. Specimen mass loss after fire exposure.

Initially, the test results indicated that the inclusion of EPS led to a significant reduction in the compressive strength. A decrease of approximately 32.9% in compressive strength was noted with a 20% EPS content, while the reduction increased to 47.9% with a 40% EPS content. The addition of steel fibers resulted in a relatively minor increase in compressive strength [4], as illustrated in Figure 3. Furthermore, the results displayed in Figure 3 and Table IV revealed that the residual compressive strength declined significantly due to the burning process. The residual compressive strength measured at 700 °C showed values of 68.3%, 81.5%, 72.9%, 67.1%, 70.7%, 67.2%, and 61.7% for *R* and the respective replacement ratio samples of group one and group two. As for the mass loss, the results indicated a further decline in residual compressive strength when incorporating steel fiber in the concrete mixtures. The mass loss increased by 14.4% and 9% due to the steel fiber inclusion for the mixtures with 20% and 40% EPS content, respectively.

TABLE IV. DETAILS OF RESIDUAL COMPRESSIVE STRENGTH VERSUS TEMPERATURE

Mix designation	Unburned samples,		Burned samples		
	F_{cu} (MPa)	%Variation	F_{cu} (MPa)	%Loss	% Residual
Group one					
R	57.1	---	39	31.7	68.3
EPS20SF0	38.3	-32.9	31.2	18.5	81.5
EPS20SF0.5	41.4	-27.5	30.2	27.1	72.9
EPS20SF1	43.7	-23.5	29.3	32.9	67.1
Group two					
R	57.1	---	39	31.7	68.3
EPS40SF0	30.0	-47.9	21.2	29.3	70.7
EPS40SF0.5	32.3	-43.4	21.7	32.8	67.2
EPS40SF1	37.6	-34.2	23.2	38.3	61.7

Concrete compressive strength experiences a sharp decline when exposed to high temperatures due to several reasons. One key factor is the dehydration of concrete, which results in the loss of free water, interlayer water, and chemically combined water that are vital for the strength and bonding of the concrete matrix. Another factor is the thermal expansion of concrete and its components, which induces internal stress and cracks that weaken the structural integrity. Additionally, the chemical decomposition of certain concrete constituents, such as calcium hydroxide and calcium silicate hydrate, diminishes the cementitious properties of the concrete [28, 29].

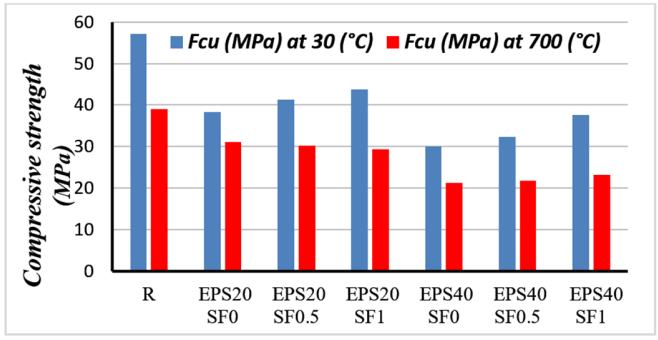

Fig. 3. Residual compressive strength versus temperature.

3) *Splitting Tensile Strength*

The split tensile strength tests were performed on fourteen standard cylinder specimens measuring 150 mm × 300 mm,

following the guidelines of ASTM C496/C496M-17 [30]. The results for the splitting tensile strength were obtained by calculating the average of two specimens tested for each mix before and after the fire exposure. The tests were conducted using a compression testing machine, where the load was applied diametrically along the length of the specimens until failure occurred. The splitting tensile strength was determined using:

$$ft = \frac{2P}{\pi DL} \quad (1)$$

where P is the applied load, D is the cylinder diameter, and L is the length of the cylinder.

Figure 4 presents the tensile strength test results for each specimen. Table V illustrates the variation in the tensile strength related to the EPS, steel fiber content, and temperature effect. The test findings indicated a significant reduction in splitting tensile strength with the addition of EPS beads. The presence of 20% and 40% EPS content led to reduction in split tensile strength of 35.20% and 40%, respectively. This result is due to the reduced splitting mechanism in lightweight concrete, as the modulus of EPS is very low compared to that of the concrete matrix, especially at higher EPS percentages [8].

The addition of steel fiber had a positive effect, resulting in a significant increase in splitting tensile strength with an increasing fiber content. Furthermore, Table V outlines the retention of tensile strength in the burned specimens. As seen in Figure 4, the tensile strength of the specimens diminished markedly due to the burning temperature. The residual tensile strengths at 700°C were 74%, 64.8%, 59.7%, 51.6%, 63.3%, 64.3%, and 58.9% for R and the respective replacement ratio samples of group one and group two. Moreover, the outcomes indicated that increasing steel fiber content resulted in a rapid decrease in the residual tensile strength of the samples exposed to fire. The tensile strength loss increased by 13.2% and 4.4% due to the steel fiber inclusion for mixtures with 20% and 40% EPS content, respectively. This is due to the high thermal conductivity of steel fibers that mitigates the EPS thermal insulation and results in an additional strength loss. It is noted that unlike the pre-fire stage, where increasing the EPS percent significantly reduced the fracture strength, after burning, an improved residual splitting strength was observed, corresponding to the increasing the EPS percent, due to its potential for enhanced thermal resistance and structural integrity in fire-prone environments [20].

TABLE V. RESIDUAL SPLITTING TENSILE STRENGTH

Mix designation	Unburned samples,		Burned samples		
	F_t (MPa)	%Variation	F_t (MPa)	%Loss	% Residual
Group one					
R	5.00	---	3.70	26.0	74.0
EPS20SF0	3.24	-35.2	2.10	35.2	64.8
EPS20SF0.5	3.85	-23.0	2.30	40.3	59.7
EPS20SF1	4.98	-2.00	2.57	48.4	51.6
Group two					
R	5.00	---	3.70	26.0	74.0
EPS40SF0	3.00	-40.0	1.90	36.7	63.3
EPS40SF0.5	3.28	-34.4	2.11	35.7	64.3
EPS40SF1	3.84	-23.2	2.26	41.1	58.9

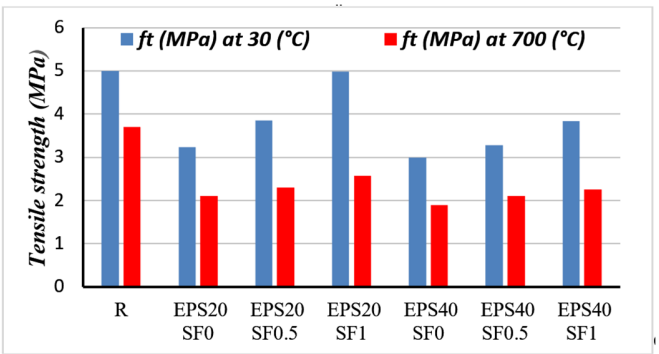

Fig. 4. Residual split tensile strength versus temperature.

4) Flexural Strength (Modulus of Rupture)

In accordance with ASTM C78/C78M-18 [31], the modulus of rupture was evaluated by testing prism specimens measuring 100 mm × 100 mm × 500 mm. The flexural strength was derived from the average of two tested specimens for each mix before and after fire exposure. The prisms underwent mid-span point loading using a flexural testing machine. The test results indicated that cracking was initiated at the tension face of the prism at the mid-span. Consequently, the modulus of rupture (fr) was calculated as:

$$fr = \frac{3P*L}{2b*d^2} \quad (2)$$

where P is the rupture load, L is the loading span, b is the prism width, and d is the prism depth.

The research findings, shown in Figure 5 and Table VI, indicated that the modulus of rupture significantly decreased with the incorporation of EPS particles, with reductions of approximately 22.2% and 30.4% observed for EPS contents of 20% and 40%, respectively.

TABLE VI. RESIDUAL FLEXURAL STRENGTH

Mix designation	Unburned samples		Burned samples		
	F_r (MPa)	%variation	F_r (MPa)	% Loss	% Residual
Group one					
R	6.35	---	4.80	-24.4	-24.4
EPS20SF0	4.94	-22.20	3.52	-28.7	-28.7
EPS20SF0.5	5.73	-9.800	3.9	-31.9	-31.9
EPS20SF1	7.95	25.20	5.26	-34.0	-34.0
Group two					
R	6.35	---	4.80	-24.4	75.6
EPS40SF0	4.42	-30.40	3.16	-28.5	71.5
EPS40SF0.5	4.95	-22.04	3.40	-31.3	68.7
EPS40SF1	7.55	18.90	5.03	-33.4	66.6

Furthermore, the addition of steel fibers led to a significant improvement in the modulus of rupture. These results align with those of previous studies [5, 6]. For specimens exposed to fire, Table VI illustrates the retention of flexural strength in the burned samples. As depicted in Figure 5, there is a considerable reduction in the flexural strength of the specimens due to exposure to elevated temperature, with a maximum loss of about 34%. Also, the residual flexural strengths at 700°C were 75.6%, 71.3%, 68.1%, 66%, 63.3% for R and the respective replacement ratio samples of group one. Similar residual

strengths ratios were noticed for group two. These results displayed an additional strength loss due to the fire exposure when the steel fibers increased for samples with different EPS ratios. This indicated that the EPS thermal insulation was diminished due to the high thermal conductivity of steel fibers that accelerate the residual flexural strength loss.

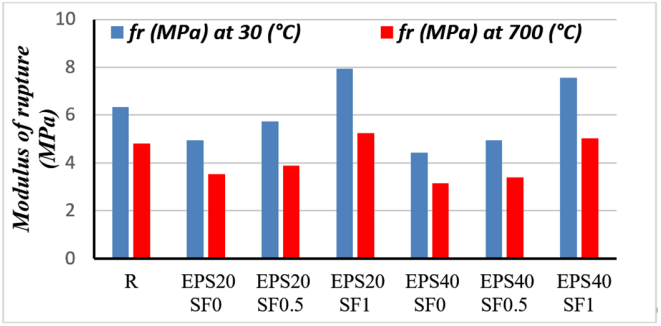

Fig. 5. Residual flexural strength versus temperature.

5) Thermal Conductivity

The thermal Conductivity test was conducted on 100 mm cubes using a Quick Thermal Conductivity Meter (QTM-500) in accordance with ACI 207.4R-20 [32], as portrayed in Figure 6.

Fig. 6. Thermal conductivity test.

The thermal conductivity of concrete is influenced by the thermal properties of its constituent phases, particularly the paste and aggregates. Aggregates constitute approximately 70% of the concrete volume, and thus replacing them with low thermal conductivity aggregates can significantly enhance the thermal insulation properties of concrete [33, 34]. Table VII presents the experimental results for the thermal conductivity of all mixes. The findings indicated that increasing the EPS content reduces the thermal conductivity of the concrete, thereby improving its thermal insulation. An enhancement of about 37% in thermal insulation was achieved when 40% of the gravel volume was replaced with EPS beads. The enhanced thermal insulation is primarily attributed to the low thermal conductivity of the trapped air within the porous structure of the EPS [35, 36]. However, the results exhibited the adverse effect of the steel fiber on the samples' thermal insulation, as their higher thermal conductivity increases the overall thermal conductivity of the concrete mixtures. An increase of 42.3%-47.7% in the thermal conductivity was noticed due to the 1% of steel fibers incorporated in the concrete mixture.

TABLE VII. CONCRETE THERMAL CONDUCTIVITY

Mix designation	Thermal conductivity (W/m-K)	Variation with R mix (%)	Variation due to EPS (%)	Variation due to steel fiber (%)
R	1.1890	----	----	
EPS20SF0	1.1573	-2.7	-2.7	----
EPS20SF0.5	1.4089	18.5		21.7
EPS20SF1	1.7091	43.7		47.7
EPS40SF0	0.7446	-37.4	-37.4	----
EPS20SF0.5	0.9552	-19.7		28.3
EPS20SF1	1.0596	-10.9		42.3

IV. CONCLUSIONS

Based on the experimental findings and analysis, the main conclusions of the present study can be summarized as:

- The results indicated that the inclusion of Expanded Polystyrene (EPS) does not affect the rheological properties of Self-Compacting Concrete (SCC). However, adding steel fiber resulted in reduced workability, which suggests a decrease in flowability, though it remained within the EFNARC limits.
- The density tests demonstrated a significant decrease when EPS was used, while adding steel fibers contributed to a slight increase in density. Overall, concrete incorporating 20% and 40% EPS breads with steel fiber can be classified as structural lightweight concrete.
- After exposure to high temperature, the observed mass loss percentages were 4.1% to 9.3%. The results indicated an additional increase in mass loss when incorporating steel fiber in the concrete mixture.
- The test results revealed a substantial reduction in the compressive strength due to the EPS beads, showing reductions of 33% and 48% for EPS contents of 20% and 40%, respectively. Moreover, the compressive strength declined significantly due to the burning process, revealing a minimum residual compressive strength of 61.7%.
- The findings indicated that the splitting tensile strength decreased with the addition of EPS beads, however adding 1% of steel fiber resulted in the restoration of tensile strength by up to 53.7% for 20% EPS. Furthermore, the tensile strength diminished markedly due to the burning, with a minimum residual tensile strength of 51.6% and 58.9% for 20% and 40% EPS content, respectively.
- The flexural strength tests showed that the modulus of rupture decreased by 22.2% and 30.4% for 20% and 40% EPS, respectively. However, the results were significantly improved by steel fiber, revealing a restoration of the flexural strength by up to 70.8% for 40% EPS. Furthermore, a considerable reduction in the flexural strength was observed due to the exposure to elevated temperature, with a maximum loss of about 34% for different EPS and steel fiber percent.

- As for the thermal properties, it was demonstrated that the EPS content significantly enhances the thermal insulation of the concrete mixture. The thermal conductivity improved by 37.4% due 40% of EPS. On the other hand, an adverse effect was noticed owing to the steel fiber inclusion.

REFERENCES

[1] A. W. Ali and N. M. Fawzi, "Production of Light Weight Foam Concrete with Sustainable Materials," *Engineering, Technology & Applied Science Research*, vol. 11, no. 5, pp. 7647–7652, Oct. 2021, https://doi.org/10.48084/etasr.4377.

[2] *Guide for Structural Lightweight Aggregate Concrete*, ACI PRC-213-14(23), American Concrete Institute, Michigan, USA, Jan. 1987.

[3] S. M and Z. K. Abbas, "The Use of Lightweight Aggregate in Concrete: A Review," *Journal of Engineering*, vol. 28, no. 11, pp. 1–13, Nov. 2022, https://doi.org/10.31026/j.eng.2022.11.01.

[4] R. K. Rakaa and R. M. Abbas, "Mechanical Properties of Lightweight EPS Self-compacting Concrete Reinforced with Steel Fibers," *Journal of Engineering*, vol. 30, no. 06, pp. 125–140, June 2024, https://doi.org/10.31026/j.eng.2024.06.08.

[5] Y. R. Maktoof and R. M. Abbas, "Effect of hybrid fibers on the performance of lightweight expanded polystyrene self-compacting concrete," in *AIP Conference Proceedings*, Dhi-Qar, Iraq, 2025, Art. no. 110014, vol. 3303, https://doi.org/10.1063/5.0261977.

[6] R. M. Abbas and R. K. Rakaa, "Structural Performance of Lightweight Fiber Reinforced Polystyrene Aggregate Self-Compacted Concrete Beams," *Engineering, Technology & Applied Science Research*, vol. 13, no. 5, pp. 11865–11870, Oct. 2023, https://doi.org/10.48084/etasr.6217.

[7] N. Liu and B. Chen, "Experimental study of the influence of EPS particle size on the mechanical properties of EPS lightweight concrete," *Construction and Building Materials*, vol. 68, pp. 227–232, Oct. 2014, https://doi.org/10.1016/j.conbuildmat.2014.06.062.

[8] R. Le Roy, E. Parant, and C. Boulay, "Taking into account the inclusions' size in lightweight concrete compressive strength prediction," *Cement and Concrete Research*, vol. 35, no. 4, pp. 770–775, Apr. 2005, https://doi.org/10.1016/j.cemconres.2004.06.002.

[9] S. Mindess, J. F. Young, and D. Darwin, *Concrete*, 2nd ed. Upper Saddle River, NJ: Prentice Hall, 2003.

[10] P. K. Mehta and P. J. M. Monteiro, *Concrete: microstructure, properties, and materials*, Fourth edition. New York: McGraw-Hill Education, 2014.

[11] J. Ko, D. Ryu, and T. Noguchi, "The spalling mechanism of high-strength concrete under fire," *Magazine of Concrete Research*, vol. 63, no. 5, pp. 357–370, May 2011, https://doi.org/10.1680/macr.10.00002.

[12] T. Drzymała, W. Jackiewicz-Rek, J. Gałaj, and R. Šukys, "Assessment of Mechanical Properties of High Strength Concrete (HSC) After Exposure to High Temperature," *Journal of Civil Engineering and Management*, vol. 24, no. 2, pp. 138–144, Apr. 2018, https://doi.org/10.3846/jcem.2018.457.

[13] M.-X. Xiong and J. Y. Richard Liew, "Spalling behavior and residual resistance of fibre reinforced Ultra-High performance concrete after exposure to high temperatures," *Materiales de Construcción*, vol. 65, no. 320, Dec. 2015, Art. no. e071, https://doi.org/10.3989/mc.2015.00715.

[14] V. K. R. Kodur and M. B. Dwaikat, "Effect of Fire Induced Spalling on the Response of Reinforced Concrete Beams," *International Journal of Concrete Structures and Materials*, vol. 2, no. 2, pp. 71–81, Dec. 2008, https://doi.org/10.4334/ijcsm.2008.2.2.071.

[15] A. Seitllari and M. Z. Naser, "Leveraging artificial intelligence to assess explosive spalling in fire-exposed RC columns," *Computers and Concrete*, vol. 24, no. 3, pp. 271–282, Sept. 2019, https://doi.org/10.12989/CAC.2019.24.3.271.

[16] B. Chen and J. Liu, "Residual strength of hybrid-fiber-reinforced high-strength concrete after exposure to high temperatures," *Cement and Concrete Research*, vol. 34, no. 6, pp. 1065–1069, June 2004, https://doi.org/10.1016/j.cemconres.2003.11.010.

[17] P. Zhang, L. Kang, J. Wang, J. Guo, S. Hu, and Y. Ling, "Mechanical Properties and Explosive Spalling Behavior of Steel-Fiber-Reinforced Concrete Exposed to High Temperature—A Review," *Applied Sciences*, vol. 10, no. 7, Mar. 2020, Art. no. 2324, https://doi.org/10.3390/app10072324.

[18] A. A. Sayadi, J. V. Tapia, T. R. Neitzert, and G. C. Clifton, "Effects of expanded polystyrene (EPS) particles on fire resistance, thermal conductivity and compressive strength of foamed concrete," *Construction and Building Materials*, vol. 112, pp. 716–724, June 2016, https://doi.org/10.1016/j.conbuildmat.2016.02.218.

[19] F. Aslani and G. Ma, "Normal and High-Strength Lightweight Self-Compacting Concrete Incorporating Perlite, Scoria, and Polystyrene Aggregates at Elevated Temperatures," *Journal of Materials in Civil Engineering*, vol. 30, no. 12, Dec. 2018, https://doi.org/10.1061/(asce)mt.1943-5533.0002538.

[20] A. Y. F. Ali, S. A. Ahmed, and M. S. El-Feky, "Alkali-activated concrete with expanded polystyrene: A lightweight, high-strength solution for fire resistance and explosive protection," *Journal of Building Engineering*, vol. 99, Apr. 2025, Art. no. 111648.

[21] *Specification and Guidelines for Self-Compacting Concrete*, EFNARC, European Federation of Producers and Applicators of Specialist Products for Structure, Switzerland, May 2005.

[22] *Test Methods for Fire Tests of Building Construction and Materials*, ASTM E119-20, ASTM International, West Conshohocken, PA, 2015, https://doi.org/10.1520/e0119-15.

[23] E. M. Mahmood, T. H. Ibrahim, A. A. Allawi, and A. El-Zohairy, "Experimental and Numerical Behavior of Encased Pultruded GFRP Beams under Elevated and Ambient Temperatures," *Fire*, vol. 6, no. 5, May 2023, Art. no. 212, https://doi.org/10.3390/fire6050212.

[24] E. M. Mahmood, A. A. Allawi, and A. El-Zohairy, "Analysis and Residual Behavior of Encased Pultruded GFRP I-Beam under Fire Loading," *Sustainability*, vol. 14, no. 20, Oct. 2022, Art. no. 13337, https://doi.org/10.3390/su142013337.

[25] S. Nagataki and H. Fujiwara, "Self-Compacting Property of Highly Flowable Concrete," in *SP-154: Advances in Concrete Technology - Proceeding Second CANMET/ ACI International Symposium*, Las Vegas, Nevada, USA, 1995, vol. 154, pp. 301–3014, https://doi.org/10.14359/960.

[26] *Building Code Requirements for Structural Concrete and Commentary*, ACI 318-19, Michigan, USA: American Concrete Institute, 2019.

[27] G. N. Narule and Y. B. Ulape, "Performance on steel fiber reinforced concrete using metakaolin," *Materials Today: Proceedings*, Apr. 2023, https://doi.org/10.1016/j.matpr.2023.04.052.

[28] R. Kuehnen, M. A. Youssef, and S. F. El-Fitiany, "Influence of Natural Fire Development on Concrete Compressive Strength," *Fire*, vol. 5, no. 2, Feb. 2022, Art. no. 34, https://doi.org/10.3390/fire5020034.

[29] Z. Guo and X. Shi, Strength of Concrete at Elevated Temperatures, Waltham, MA: Elsevier, 2011.

[30] *Test Method for Splitting Tensile Strength of Cylindrical Concrete Specimens*, ASTM C496-96, ASTM International, West Conshohocken, PA, https://doi.org/10.1520/c0496_c0496m-17.

[31] *Test Method for Flexural Strength of Concrete (Using Simple Beam with Third-Point Loading)*, ASTM C78/C78M-22, ASTM International, West Conshohocken, PA, https://doi.org/10.1520/c0078_c0078m-18.

[32] *Report on Cooling and Insulating Systems for Mass Concrete*, ACI 207 4R 20, ASTM International, West Conshohocken, PA, 2020.

[33] J. M. Chi, R. Huang, C. C. Yang, and J. J. Chang, "Effect of aggregate properties on the strength and stiffness of lightweight concrete," *Cement and Concrete Composites*, vol. 25, no. 2, pp. 197–205, Feb. 2003, https://doi.org/10.1016/s0958-9465(02)00020-3.

[34] A. M. Neville, *Properties of concrete*, 4th ed. Melbourne, Australia: Longman Australia Pty Limited, 1995.

[35] R. Demirboğa and R. Gül, "The effects of expanded perlite aggregate, silica fume and fly ash on the thermal conductivity of lightweight concrete," *Cement and Concrete Research*, vol. 33, no. 5, pp. 723–727, May 2003, https://doi.org/10.1016/s0008-8846(02)01032-3.

[36] M. Maage *et al.*, *LWAC Material Properties - State-of-the-Art*. Brussels, Belgium: Industrial and Materials Technologies Programme, European Union, 2000.